Lecture 18

Self-focusing. Self-phase modulation; spectral broadening, and supercontinuum generation. Few-cycle optical pulses generation via spectral broadening and pulse compression.

Self-focusing

In Lecture 17 we derived expressions for intensity-dependent refraction and nonlinear index n_2 (for self-action)

The ususal way of defining the intensity-dependent refractive index is by means of the equation:

linear ref. index

intensity dependent ref. index

$$n = n_0 + \underbrace{n_2 I}_{\Delta n} \qquad (17.4)$$

Hence we find that n_2 is related to $\chi^{(3)}$ by

$$\boxed{n_2 = \frac{3\chi^{(3)}}{4n_0^2\epsilon_0 c}} \qquad (17.5)$$

n_2 is usually positive

Self-focusing

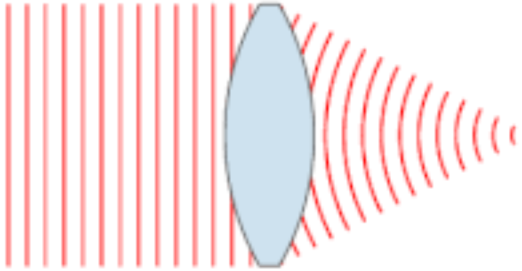

Self-focusing: 3 scenarios

n_2 is **positive** in common optical materials. As a result, the laser beam induces a refractive index variation within the material with a larger refractive index at the center of the beam than at its periphery. Thus the material acts as if it were a positive lens, causing the beam to come to a focus within the material.

Three self-action effects:

(a) self-focusing of light,

(b) self-trapping of light,

(c) laser beam breakup, showing the transverse distribution of intensity of a beam that has broken up into many filaments.

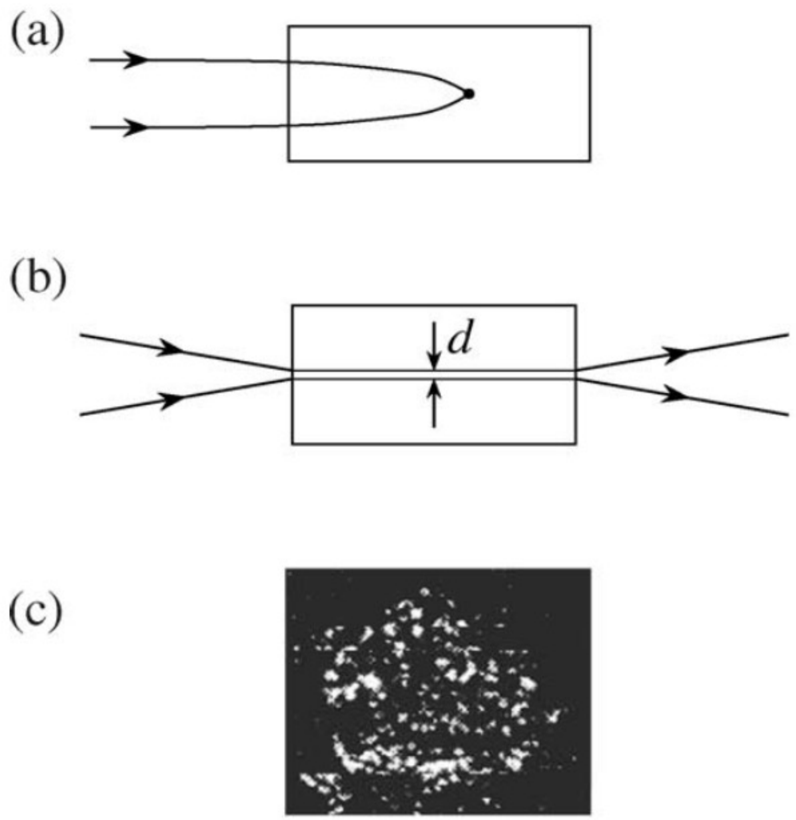

Self-focusing: a simple model

Prediction of the self-focusing distance z_{sf} by means of Fermat's principle.

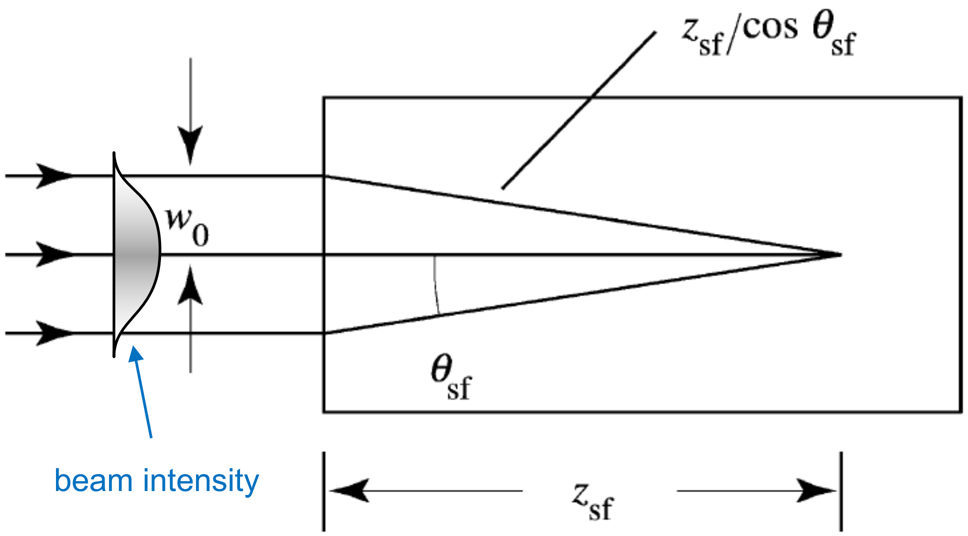

Fermat's principle tells us that $$(n_0+n_2 I)z_{sf} = n_0 z_{sf}/\cos\theta$$

$$\cos\theta \approx 1-\frac{1}{2}\theta^2 \qquad 1/\cos\theta \approx 1+\frac{1}{2}\theta^2$$

get self-focusing angle: $$\theta_{sf} = \sqrt{\frac{2n_2 I}{n_0}} = \sqrt{\frac{2\Delta n}{n_0}} \qquad (18.1)$$

this formula assumes the self-focusing effect to be large, so that diffraction is ignored

* Fermat's principle: the path taken by a ray between two given points is the path that can be traversed in the least time.

Self-focusing

Self-trapping of light – occurs when the tendency of a beam to spread as a consequence of diffraction is precisely balanced by the tendency of the beam to contract as a consequence of self-focusing.

Following Boyd textbook:

Diffraction pattern by a circular aperture diam. D

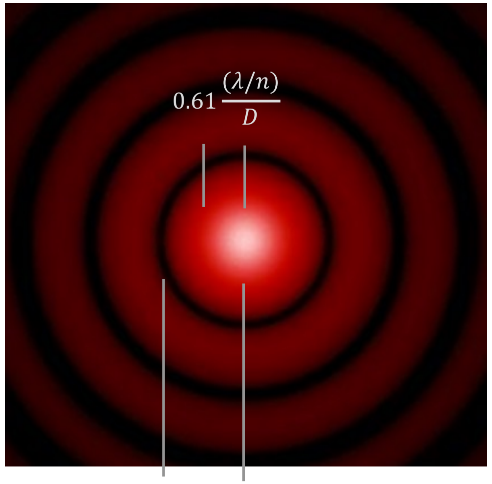

$\theta = 1.22\frac{(\lambda/n)}{D}$

→ The diffraction angle $\theta_{diff} \approx 0.61\frac{(\lambda/n_0)}{D}$ should be equal to the self-focusing angle of Eq. (18.1)

$$\theta_{sf} = \sqrt{\frac{2n_2 I}{n_0}}$$

→

$$0.61\frac{(\lambda/n_0)}{D} = \sqrt{\frac{2n_2 I}{n_0}}$$

$$I = (0.61)^2\frac{\lambda^2}{2n_0 n_2 D^2}$$

$$\boxed{P_{cr} \approx \frac{\pi D^2}{4} I \approx \frac{\pi (0.61)^2 \lambda^2}{8 n_0 n_2}} \qquad (18.2)$$

The more or less exact formula for Gaussian beams

$$\boxed{P_{cr} = \frac{1.2\lambda^2}{8 n_0 n_2}} \qquad (18.3)$$

(Fibich and Gaeta OL 25, 335, 2000)

Self-focusing: a simple model

Note that this result does not depend on the beam width, but just on the **power**. Therefore even very broad beams can eventually self-focus in a self-focusing medium if their total power exceeds P_c .

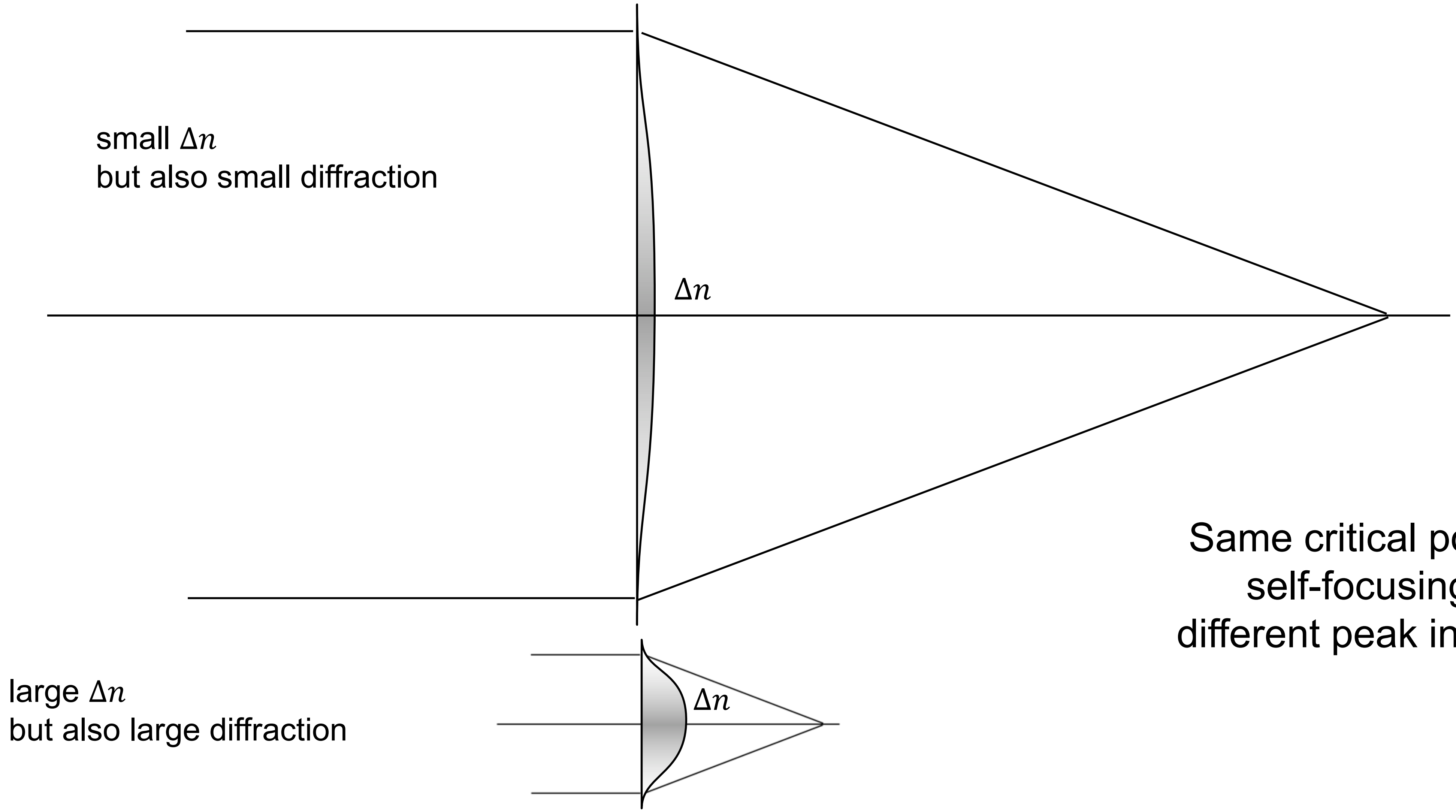

Same critical power for self-focusing but different peak intensities

Self-focusing: a simple model

More generally: the two competing processses result in the total convergence angle:

$$\theta = \sqrt{\theta_{sf}^2 - \theta_{diff}^2}$$

From (18.1) it follows that $\theta_{sf}^2 \sim I \; and \; (at \; a \; given \; beamsize) \sim P$,

hence $\theta = \theta_{diff}\sqrt{P/P_{cr} - 1}$

The characteristic self-focusing **distance** (Gaussian beams)

$$z_{sf} = \frac{w_0}{\theta} \approx \frac{w_0}{\frac{(\lambda/n)}{\pi w_0}} \frac{1}{\sqrt{P/P_{cr} - 1}} \approx \frac{\frac{\pi w_0^2}{(\lambda/n)}}{\sqrt{P/P_{cr} - 1}} = \frac{z_D}{\sqrt{P/P_{cr} - 1}}$$

Self-focusing

Yariv (1975) has shown that for **Gaussian beams** with arbitrary beam-waist position (z_{min}), the distance from the entrance face to the position of the self-focus (z_{sf}) is given by the formula

$$\boxed{z_{sf} = \frac{\frac{1}{2}kw^2}{(P/P_{cr} - 1)^{1/2} + 2z_{min}/kw_0^2}} \qquad (18.4)$$

$$k = \frac{2\pi}{\lambda/n}$$

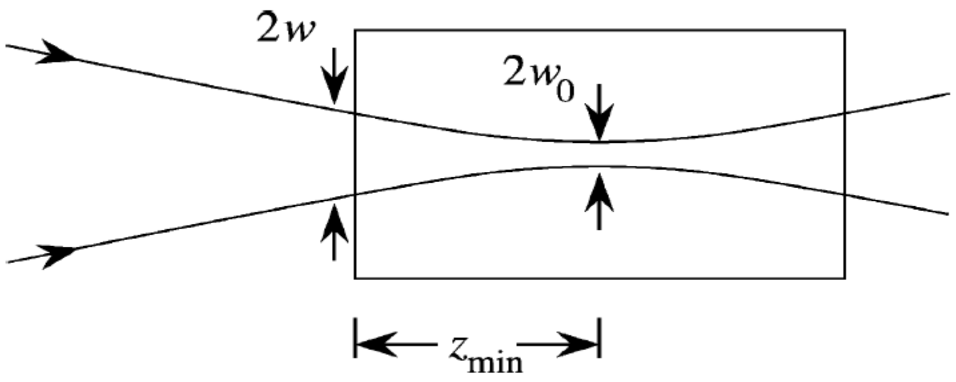

Example:
Beam waist at the front crystal surface
$w = w_0 \;\; (z_{min} = 0)$

Rayleigh length

$$z_{sf} = \frac{\frac{1}{2}kw_0^2}{(P/P_{cr} - 1)^{1/2}} = \frac{\frac{\pi w_0^2}{(\lambda/n)}}{(P/P_{cr} - 1)^{1/2}} = \frac{z_R}{(P/P_{cr} - 1)^{1/2}} \qquad (18.5)$$

0.734

(Fibich and Gaeta OL 25, 335, 2000)

$P/P_{cr}=1 \rightarrow \quad z_{sf}=\infty$ **SELF GUIDING**

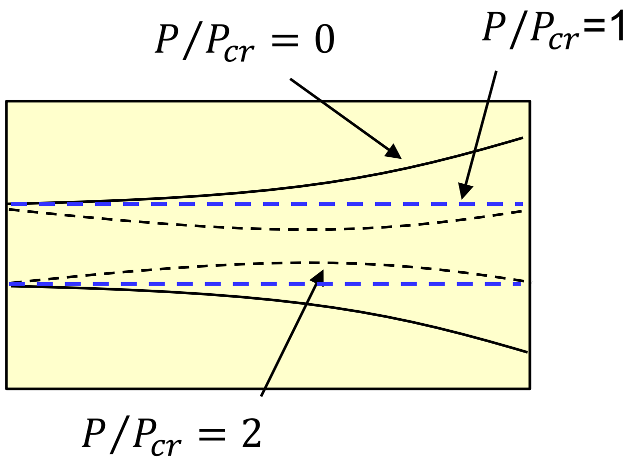

Self-focusing: another derivation for P_{cr}

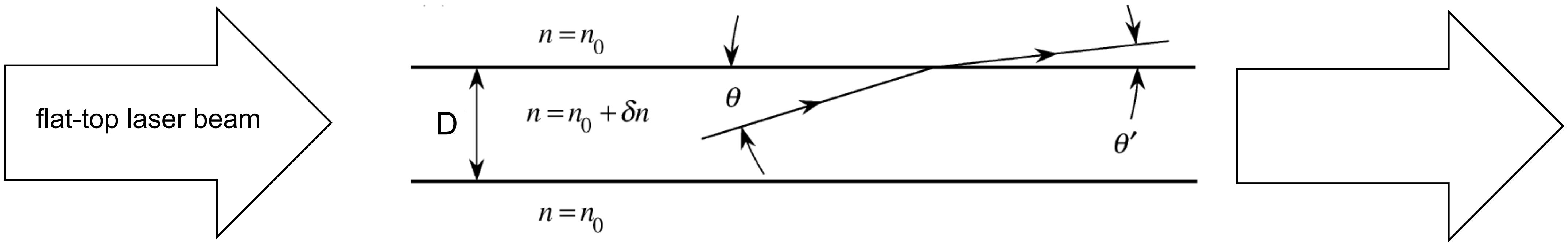

Total internal reflection occurs if θ is less than the critical angle θ_0 for total internal reflection, which is given by

$$\cos\theta_0 = \frac{n_0}{n_0 + \delta n}.$$

This can be approximated by: $1 - \frac{1}{2}\theta_0^2 = 1 - \frac{\delta n}{n_0},$ hence $\theta_0 = \sqrt{2\delta n/n_0} = \sqrt{2n_2 I/n_0}$

A laser beam of diameter D (flat-top) will contain rays within a cone whose angular extent is of the order of : $\theta_{diff} \approx 0.61\frac{(\lambda/n_0)}{D}$

Self-trapping will occur if total internal reflection occurs for all of the rays contained within the beam $\theta_{diff} = \theta_0$ hence $\sqrt{2n_2 I/n_0} = 0.61\frac{(\lambda/n_0)}{D},$ $I = \frac{(0.61)^2\lambda^2}{2n_0 n_2 D^2}$

and we get $\boxed{P_{cr} \approx \frac{\pi D^2}{4} I \approx \frac{\pi(0.61)^2\lambda^2}{8n_0 n_2}}$ (18.6) - same as (18.2)

Again, the power, not the intensity, of the laser beamis is crucial in determining whether self-focusing will occur

Self-focusing

from Lecture 17

Some examples:

1) For CS_2 n_2=3.2x10^{-18} m^2/W
$(\lambda = 1.06\ \mu m)$

$P_{cr} = \frac{\pi(0.61)^2\lambda^2}{8n_0n_2}$= 31kW

pi*0.61^2*1.06e-6^2/ 8/1.63/3.2e-18

		n_0		n_2 (cm^2/W)
	Liquids			
	Acetone	1.36	1.5×10^{-21}	2.4×10^{-15}
	Benzene	1.5	9.5×10^{-22}	1.2×10^{-15}
CS_2	Carbon disulfide	1.63	3.1×10^{-20}	3.2×10^{-14}
	CCl_4	1.45	1.1×10^{-21}	1.5×10^{-15}
	Diiodomethane	1.69	1.5×10^{-20}	1.5×10^{-14}
	Ethanol	1.36	5.0×10^{-22}	7.7×10^{-16}
	Methanol	1.33	4.3×10^{-22}	6.9×10^{-16}
	Nitrobenzene	1.56	5.7×10^{-20}	6.7×10^{-14}
	Water	1.33	2.5×10^{-22}	4.1×10^{-16}
	Other materials			
	Air	1.0003	1.7×10^{-25}	5.0×10^{-19}

Example:
1 mJ , 10 ns pulse;   P= 100kW > P_{cr}

2) For SiO_2 fiber n_2=3.2x10^{-20} m^2/W
$\lambda = 1.56\ \mu m$

$P_{cr} = \frac{\pi(0.61)^2\lambda^2}{8n_0n_2}$= 7.6 MW

pi*0.61^2*1.56e-6^2/ 8/1.47/3.2e-20

e.g. 1 μJ pulse with 100-fs duration

→ 10 MW peak power

3) For **air** n_2=5x10^{-23} m^2/W
$\lambda = 10.6\ \mu m$ (CO_2 laser)

$P_{cr} = \frac{\pi(0.61)^2\lambda^2}{8n_0n_2}$= 3.3 GW

pi*0.61^2*10.6e-6^2/ 8/1/5e-23

e.g. need 3.3 mJ pulse with 1-ps duration

Self-focusing

Kerr-lens mode locking in a Ti:sapphire laser

42 OPTICS LETTERS / Vol. 16, No. 1 / January 1, 1991

60-fsec pulse generation from a self-mode-locked Ti:sapphire laser

D. E. Spence, P. N. Kean, and W. Sibbett

J. F. Allen Physics Research Laboratories, Department of Physics and Astronomy, University of St. Andrews, North Haugh, St. Andrews, Fife, KY16 9SS, Scotland

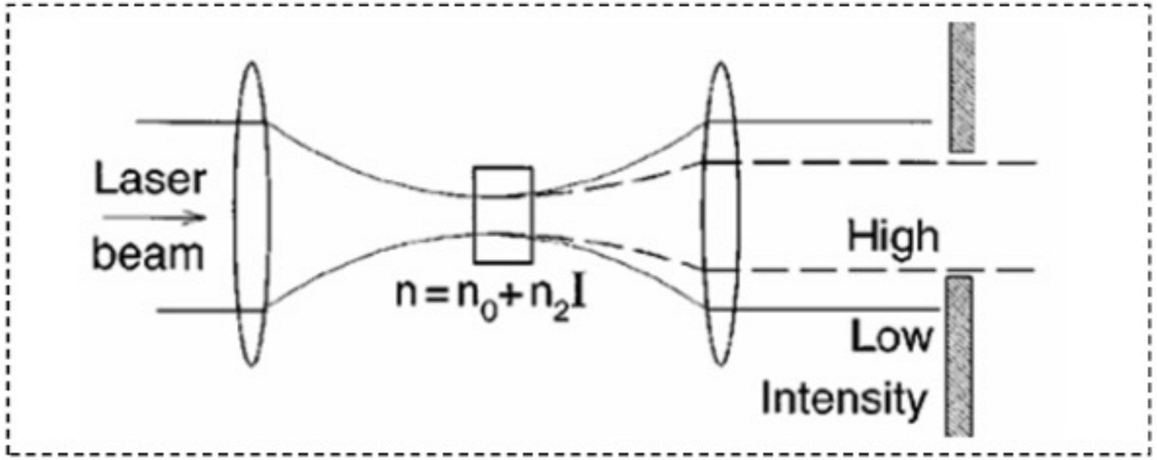

Self-phase modulation, spectral broadening, and supercontinuum generation

Spectral broadening related to short pulses

Self-phase modulation (SPM) affects the phase of an optical pulse due to the intensity-dependent refractive index

$$n(I) = n + n_2 I$$

The phase of a wave is expressed as

$$\varphi = \omega_0 t - kL + \varphi_0 \qquad k = k_0 n(I)$$

Is an intensity-dependent wavenumber

$$k_0 = \frac{2\pi}{\lambda_0}$$

vacuum *k*-vector

Therefore, the **intensity dependent phase shift** along the pulse is

$$\Delta\varphi = -\Delta k L = -k_0 \Delta n(I) L = -k_0 n_2 I L$$

Or considering the **instantaneous frequency**

$$\omega = \frac{d\varphi}{dt} = \omega_0 \underbrace{- k_0 L n_2 \frac{dI}{dt}}_{\Delta\omega}$$

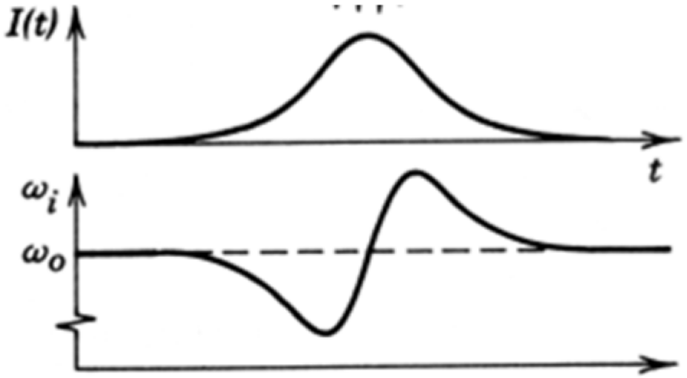

Spectral broadening

Let us look more carefully at this term, $\Delta\omega = -k_0 L n_2 \dfrac{dI}{dt}$

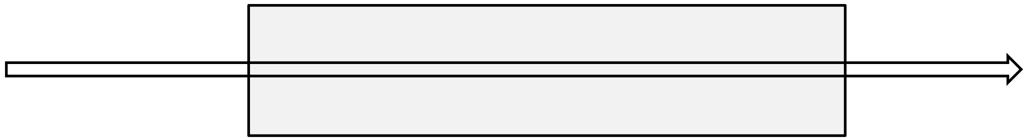

Analogy with mirror reflection:

Mirror

Mirror is stationary:
frequency ω does not change

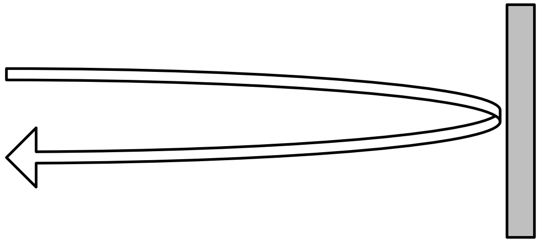

Mirror is fast moving: first away from the beam and then towards the beam. The frequency ω changes because of the Doppler effect

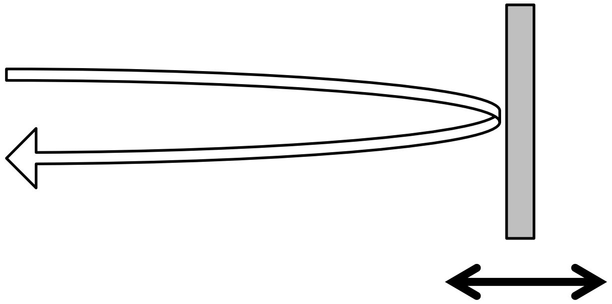

max phase shift, zero frequency shift

pulse leading edge

$\frac{dI}{dt} > 0, \quad \Delta\omega < 0$

pulse trailing edge

$\frac{dI}{dt} < 0, \quad \Delta\omega > 0$

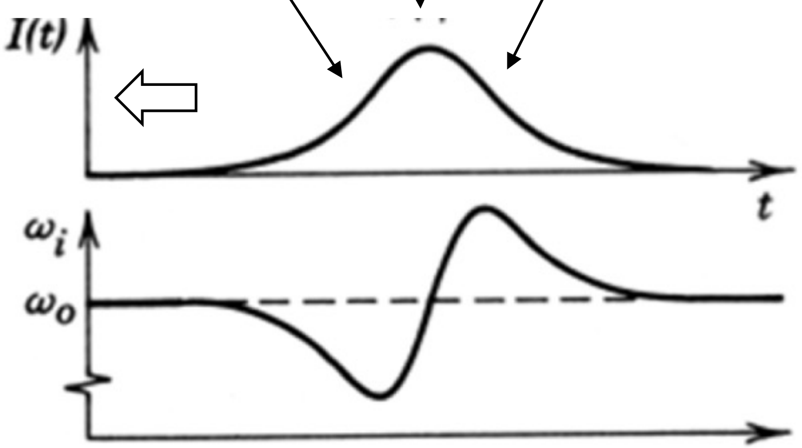

see Stegeman p.353

Spectral broadening

$$\Delta\varphi = -k_0 n_2 I_0 L$$

max. nonlinear phase shift $\Delta\varphi$ =2π

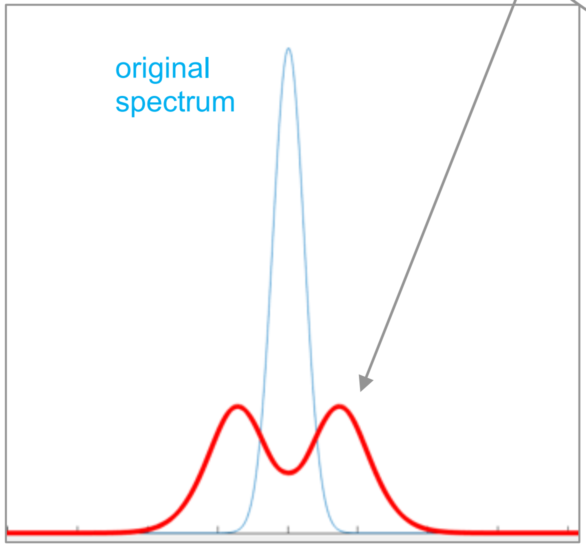

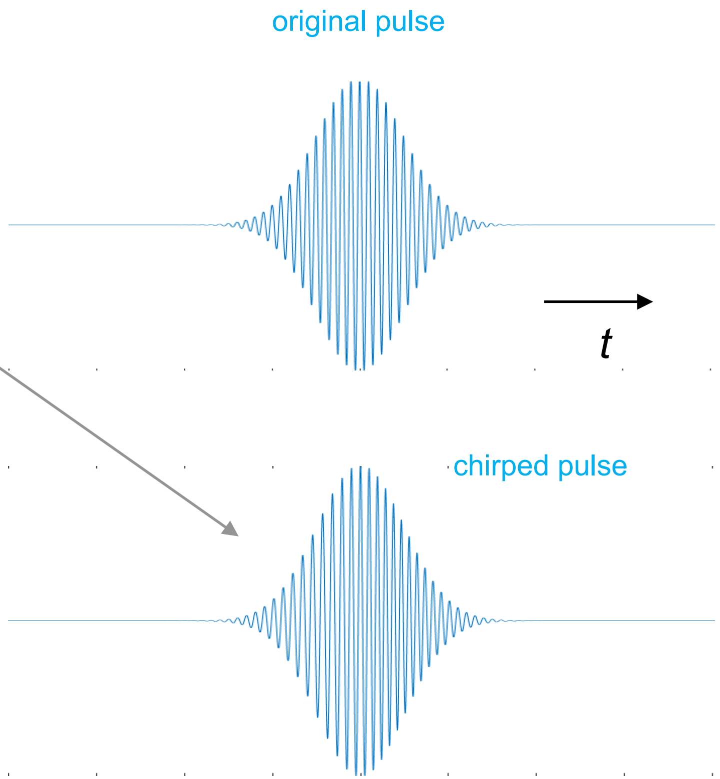

Spectral broadening

$$\Delta\varphi = -k_0 n_2 I_0 L$$

max. nonlinear phase shift $\Delta\varphi$ =10π

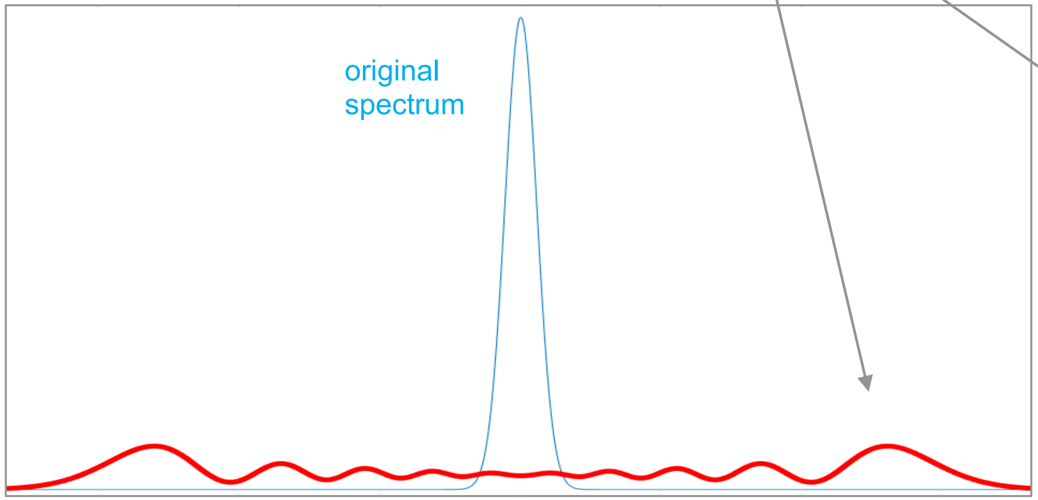

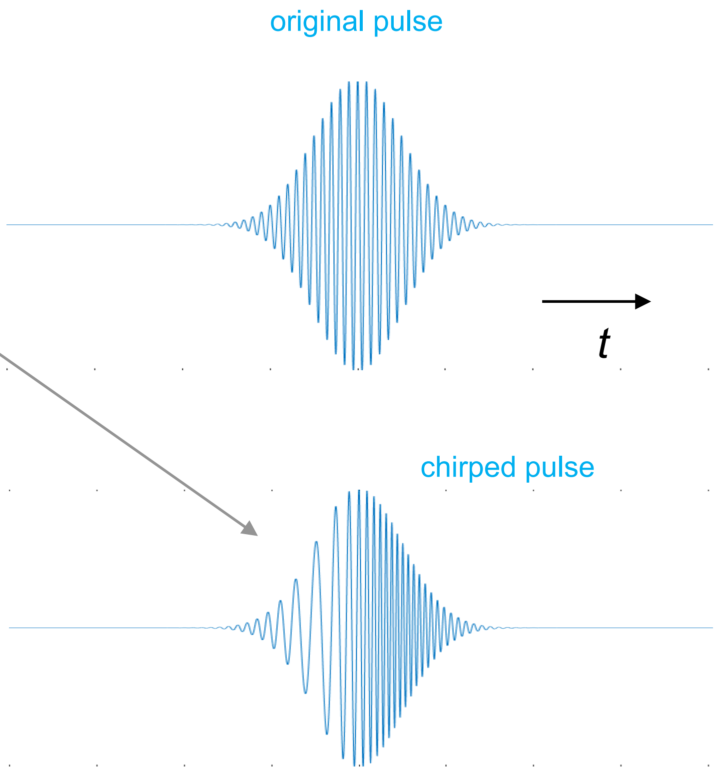

Spectral broadening

FIGURE 14.6 The evolution of the output spectrum with increasing input power and the corresponding nonlinear phase shift $\Delta\phi^{NL}(L)$. Reproduced with permission from American Physical Society (5).

R. H. Stolen and C. Lin, "Self-phase-modulation in silica optical fibers," Phys. Rev. A, **17**, 1448–1453 (1978).

G. Stegeman

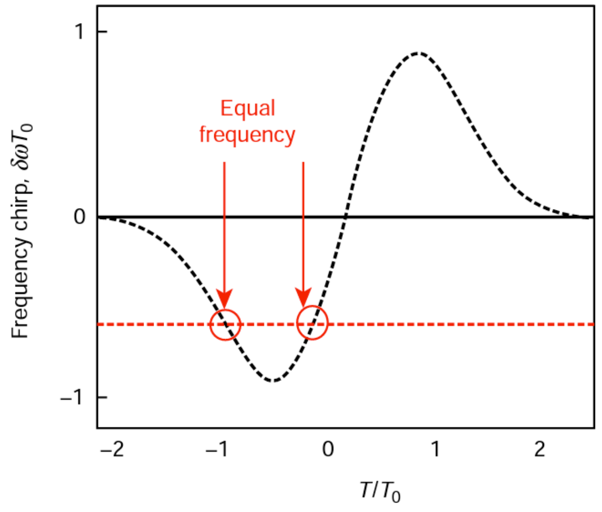

There are points on the pulse envelope that correspond to the same frequency shift; but this points are shifted in time. Hence constructive or destructive interference can occur.

Spectral broadening

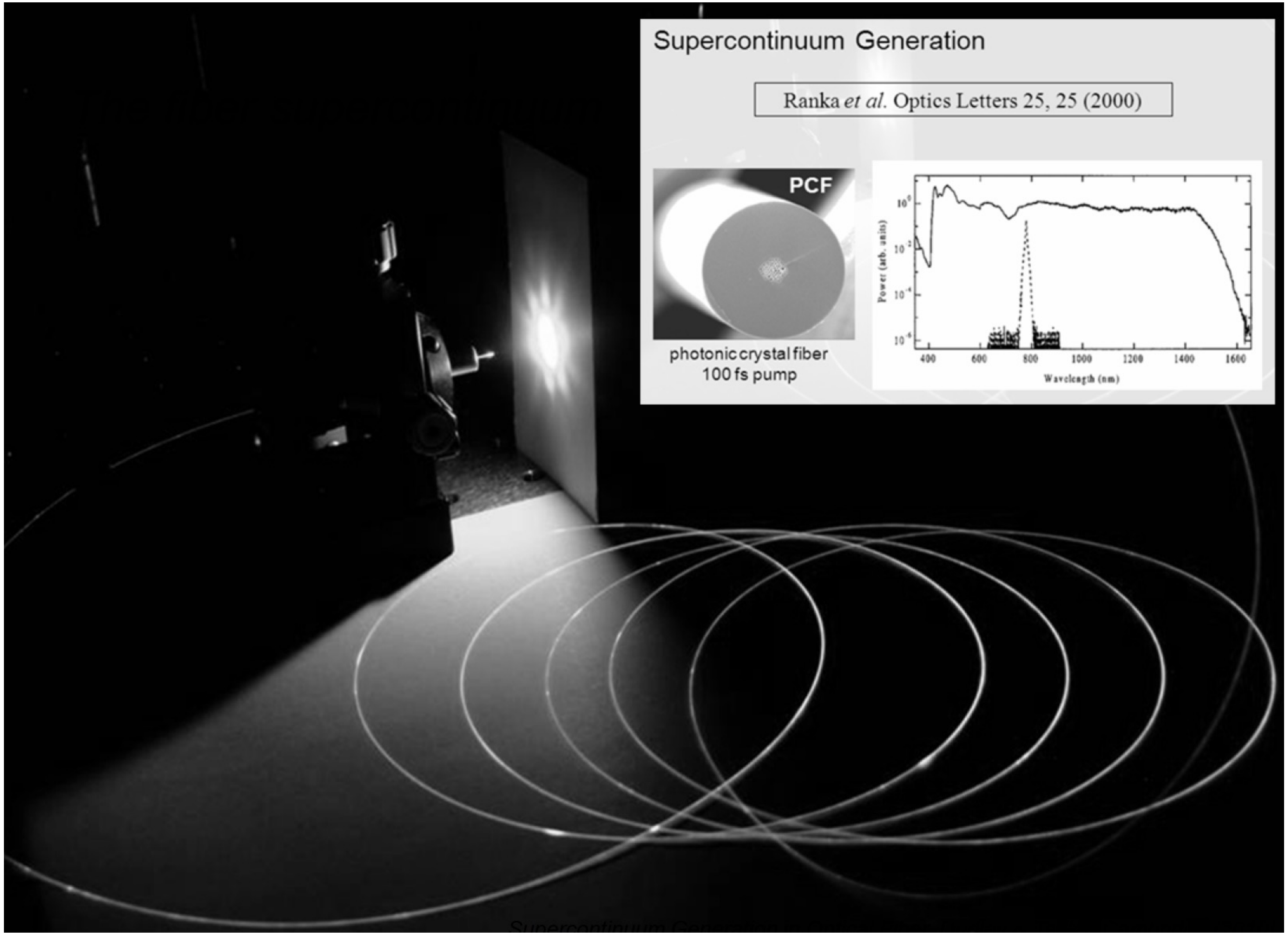

Spectral broadening

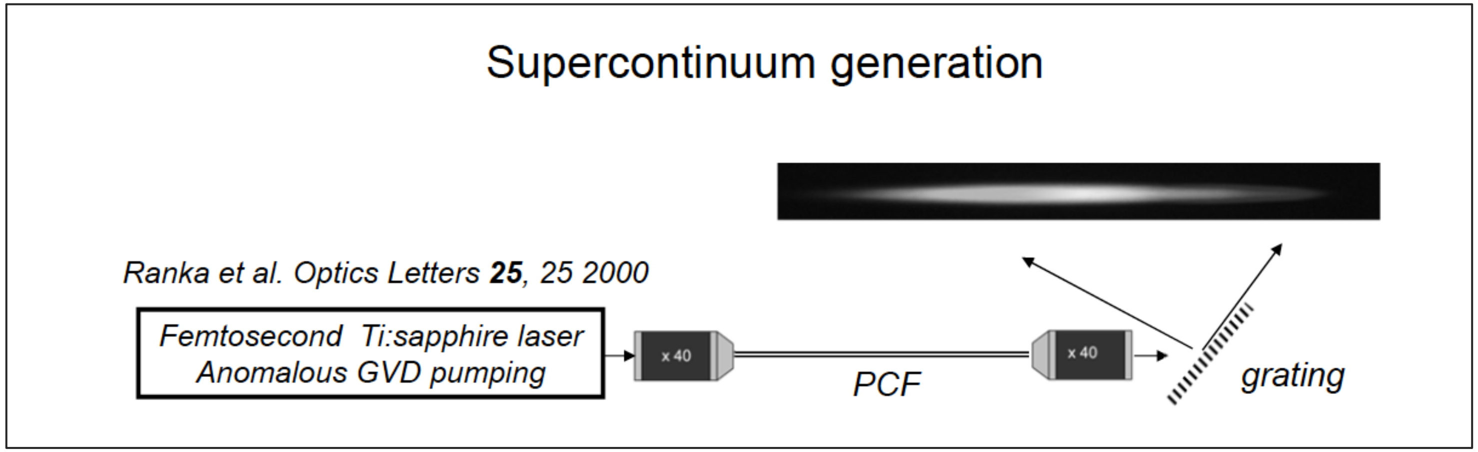

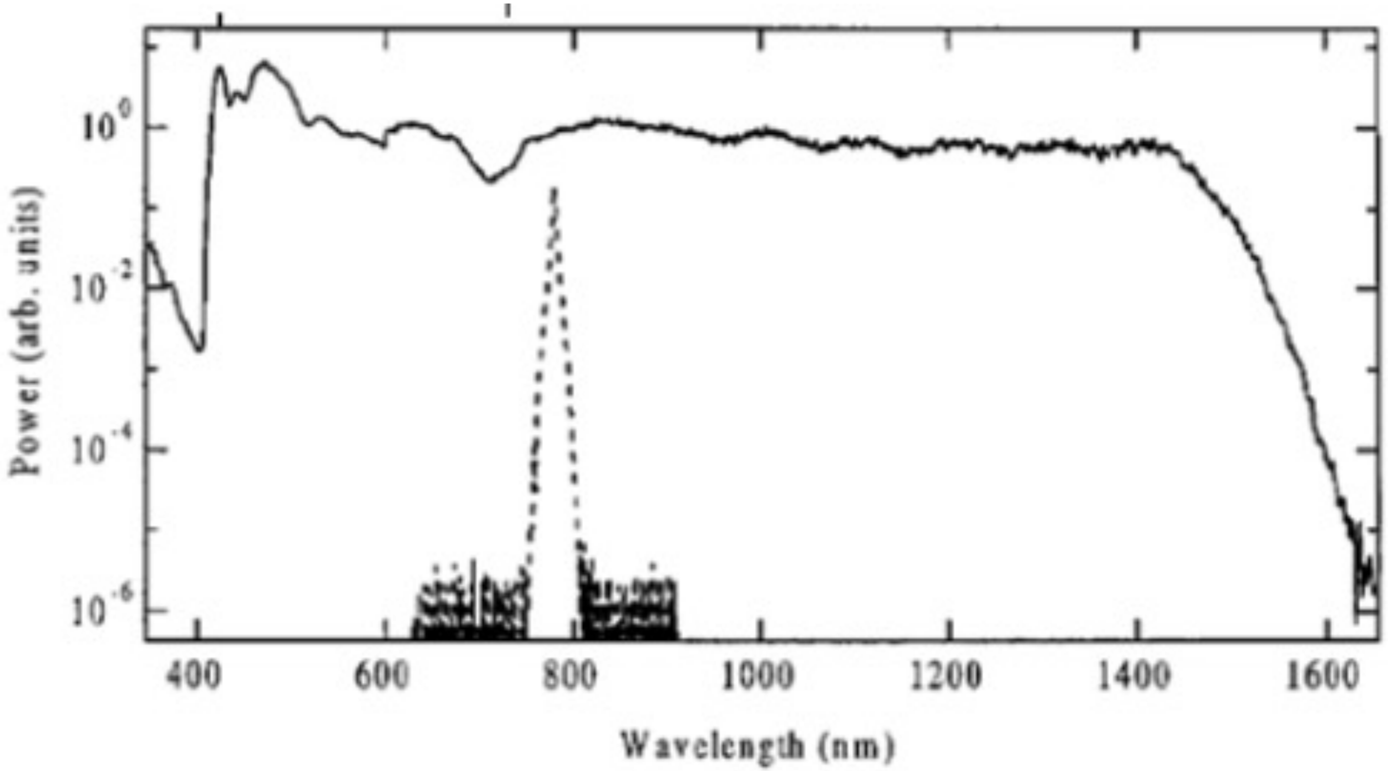

Supercontinuum generation in sub-cm segments of highly nonlinear tellurite fiber

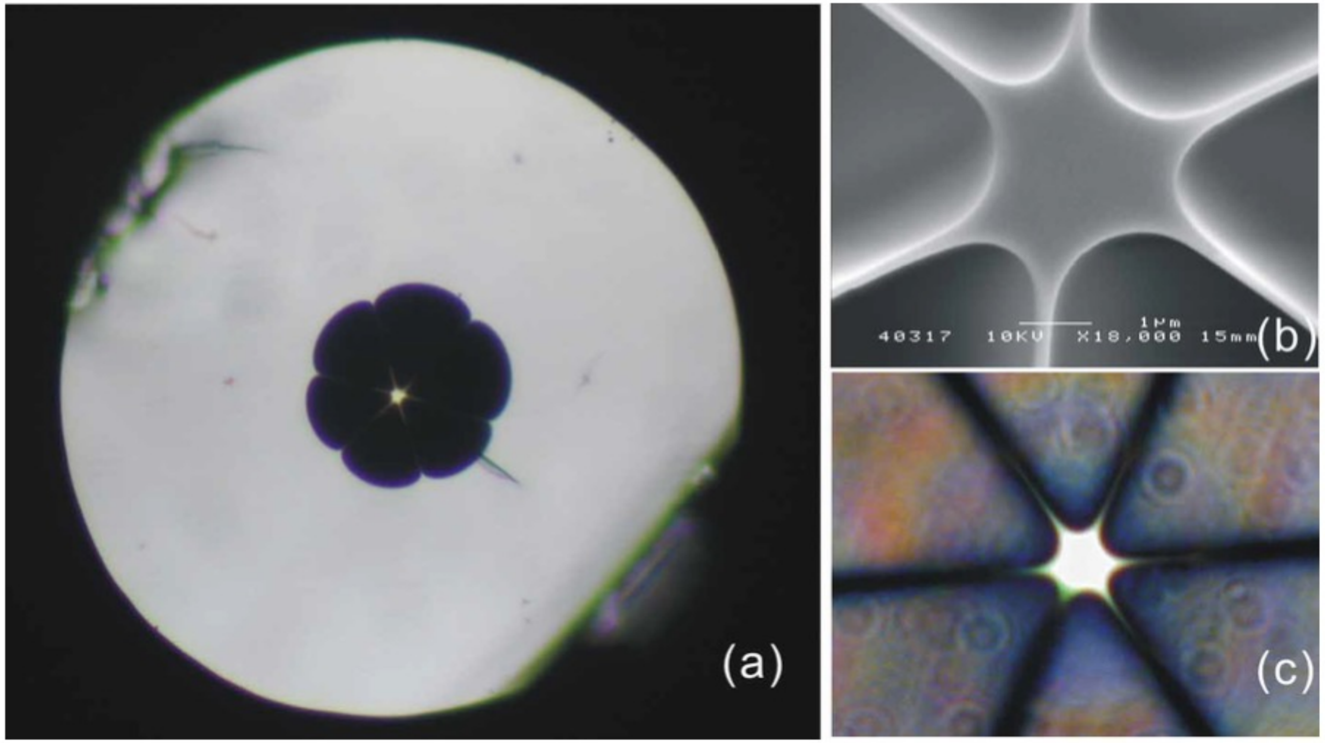

Figure 6.3 Cross sectional profile of the tellurite PCF in the optical microscopy (a, c) and electron microscopy (b). Scale bar in (b) is 1μm. Reproduced from Fig. 1 of [10] – with permission of OSA, The Optical Society.

P. Domachuk, N. A. Wolchover, M. Cronin-Golomb, A. Wang, A. K. George, C. M. B. Cordeiro, J. C. Knight, and F. G. Omenetto, Over 4000 nm bandwidth of mid-IR supercontinuum generation in sub-centimeter segments of highly nonlinear tellurite PCFs, Opt. Express 16, 7161 (2008).

Spectral broadening

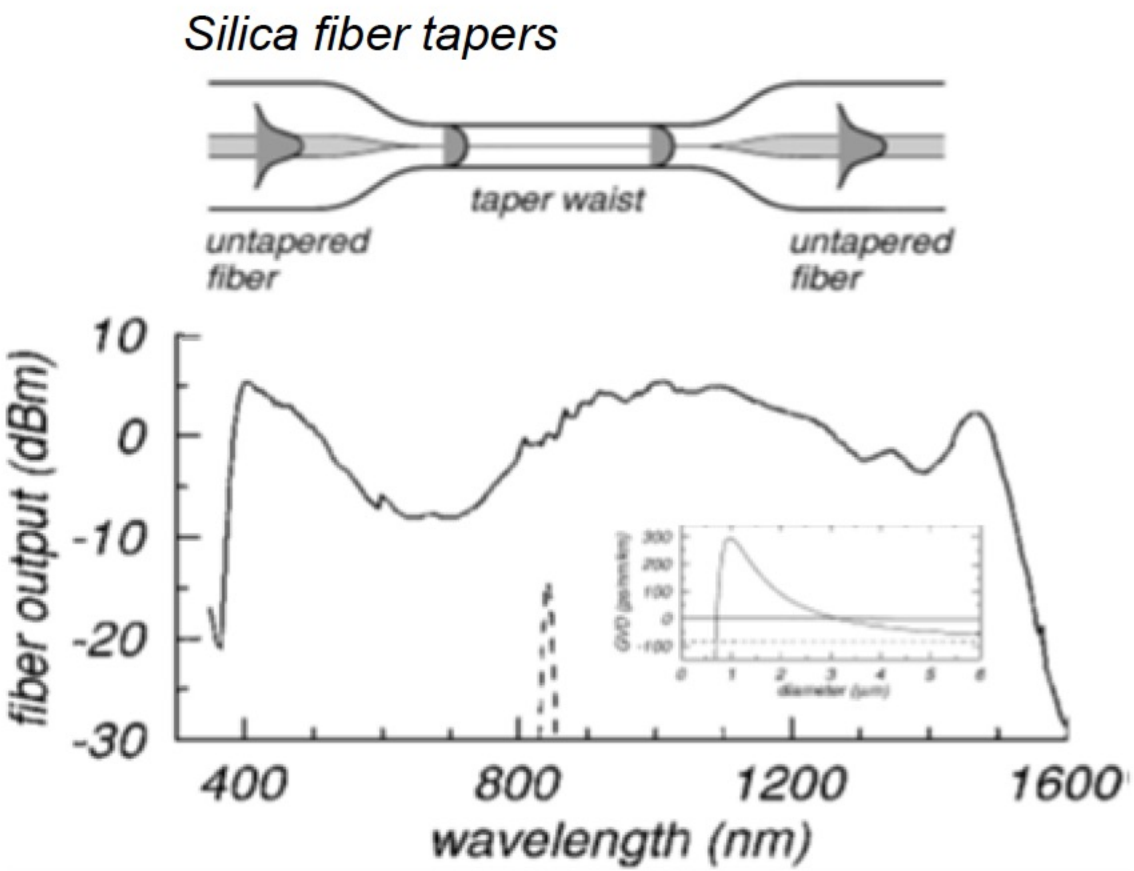

T. A. Birks et al., OL 25 1415 (2000)

Spectral broadening

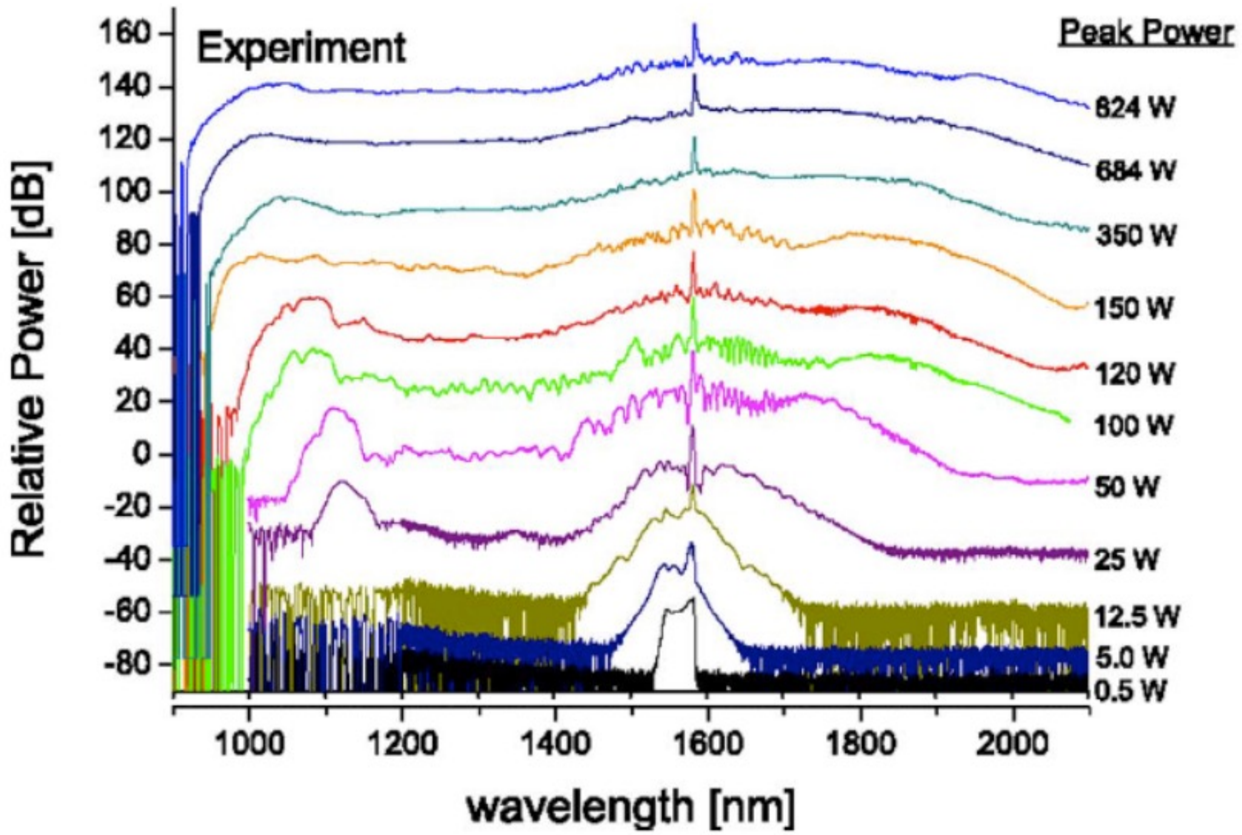

Figure 6.9 Output SC spectra from the As_2S_3 tapered fiber as a function of the peak pump power. Reproduced from Fig. 4 of [27] – with permission of OSA, The Optical Society.

D. D. Hudson, S. A. Dekker, E. C. Mägi, A. C. Judge, S. D. Jackson, E. Li, J. S. Sanghera, L. B. Shaw, I. D. Aggarwal, and B. J. Eggleton, Octave spanning supercontinuum in an As_2S_3 taper using ultralow pump pulse energy, Opt. Lett. 36, 1122 (2011).

Spectral broadening

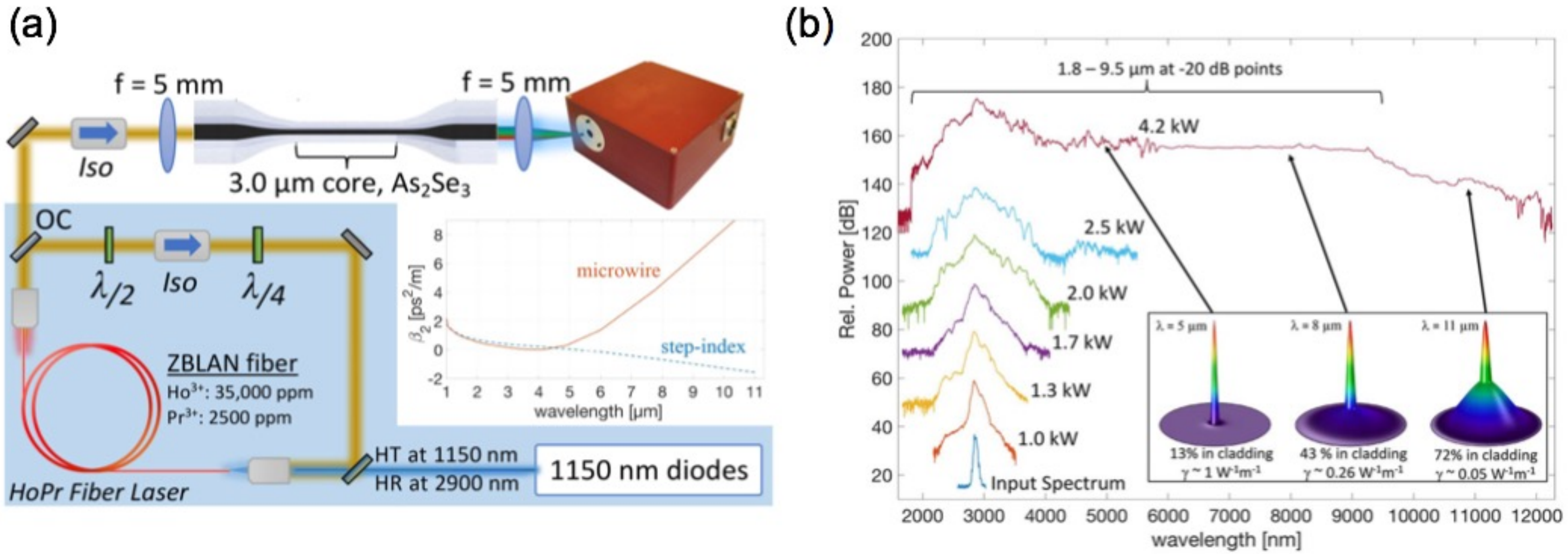

Figure 6.12 (a) Layout of the 1.8-9.5-µm supercontinuum generator [39]. The holmium laser output passes through an isolator (>40 dB suppression) and is focused into the core of the tapered fiber. The output is collected using a ZnSe lens and focused into a spectrometer. The inset shows the calculated dispersion of both the untapered step-index fiber and the microwire (tapered) section. (b) Spectral broadening as a function of the peak power (vertically offset for clarity). The inset shows the mode profile in the tapered section (3 µm core diameter), as well as the nonlinear parameter γ at various wavelengths. Reproduced from Figs. 1 and 4 of [39] – with permission of OSA, The Optical Society.

D. D. Hudson, S. Antipov, L. Li, I. Alamgir, T. Hu, M. El Amraoui, Y. Messaddeq, M. Rochette, S. D. Jackson, and A. Fuerbach, Toward all-fiber supercontinuum spanning the mid-infrared, Optica 4, 1163 (2017).

Few-cycle optical pulses generation via spectral broadening and pulse compression

Spectral broadening

For self-phase modulation to occur, the response time of the nonlinearity should be **much shorter** than the pulse width.

CS_2 case:

for fs pulses: Only fast (electron) Kerr nonlinearity would work

for > 1 ps pulses: Both vibrational and the Kerr nonlinearity would work

Pulse compression

In the absence of nonlinearity, pulse broadening always occurs due to group velocity dispersion (GVD), which is the equivalent of diffraction in the space domain.

normal dispersion:
red runs faster than blue

Pulse compression: when $n_2 > 0$ and group velocity dispersion is anomalous:

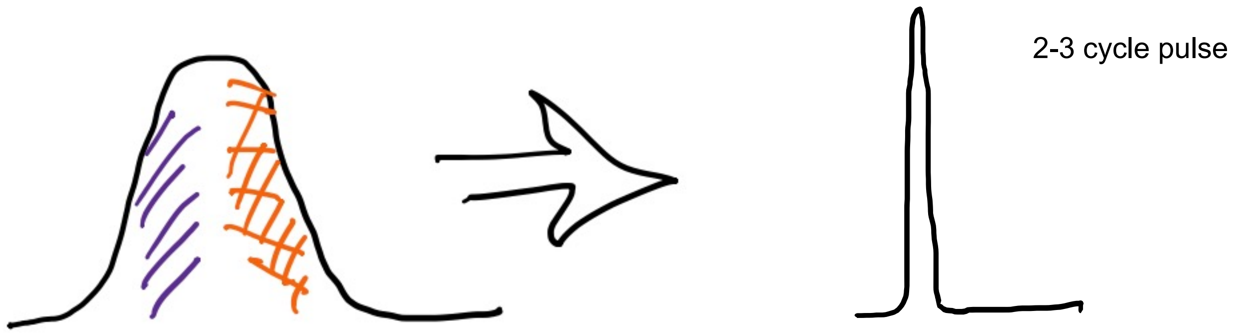

anomalous dispersion:
blue runs faster than red

Nonlinearly compressed pulses of a Kerr-lens mode-locked ytterbium-doped yttrium–aluminium–garnet (Yb:YAG) thin-disc oscillator

The initial pulses were produced by a Kerr-lens mode-locked Yb: YAG thin-disc oscillator that operates at a 100 MHz repetition rate. The oscillator delivers **250 fs** pulses at 1.03 μm and an average power of 90 W.

nature photonics | LETTERS
PUBLISHED ONLINE: 21 SEPTEMBER 2015 | DOI: 10.1038/NPHOTON.2015.179

High-power sub-two-cycle mid-infrared pulses at 100 MHz repetition rate

I. Pupeza[1,2*], D. Sánchez[2], J. Zhang[1,3], N. Lilienfein[1,4], M. Seidel[1,4], N. Karpowicz[1], T. Paasch-Colberg[4,5†], I. Znakovskaya[1,4], M. Pescher[4], W. Schweinberger[4,5], V. Pervak[4], E. Fill[1,4], O. Pronin[1,4], Z. Wei[3], F. Krausz[1,4], A. Apolonski[1,4] and J. Biegert[2,6]

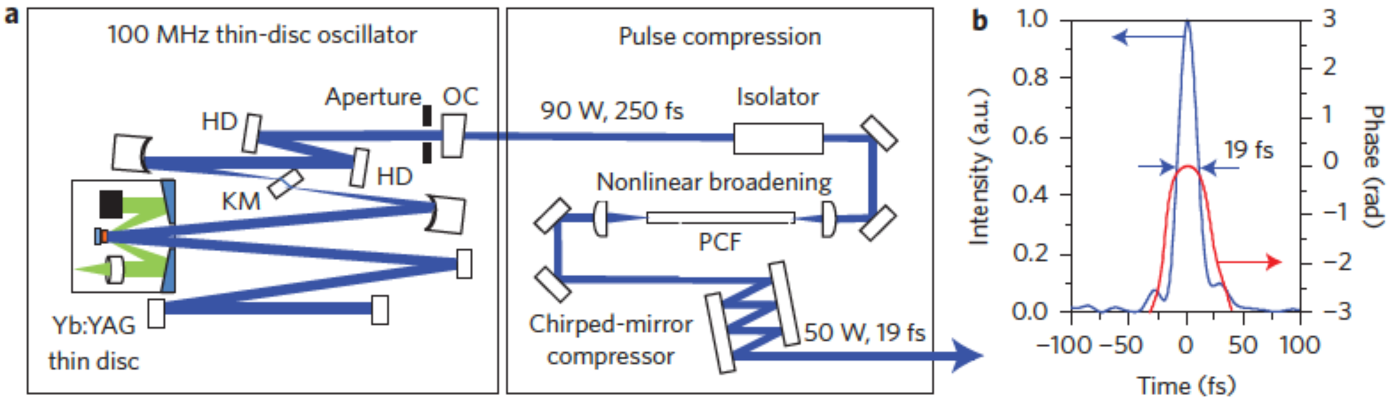

Figure 1 | Driving laser. a, Kerr-lens mode-locked Yb:YAG thin-disc oscillator. The 0.1 mm thin disc is wedged and curved with a radius of curvature of about 20 m. The disc is pumped at 940 nm in a multipass cavity configuration (green beam), which results in a pump spot diameter of 2.5 mm. The oscillator beam diameter on the disc is 2.2 mm ($1/e^2$ intensity). The 250 fs pulses (centre wavelength of 1,030 nm) produced by the oscillator are broadened to about 125 nm FWHM in an 80-mm-long large-mode-area PCF with a mode-field diameter of 35 μm. Temporal compression is subsequently achieved by 20 bounces on two types of chirped mirrors in a double-angle configuration, which accumulates a total group-delay dispersion of about $-2{,}200\ \mathrm{fs}^2$. The footprint of the oscillator and compression stage is $50\times150\ \mathrm{cm}^2$. HD, highly dispersive mirrors; OC, output coupler; KM, Kerr medium. **b**, Temporal intensity and phase of the compressed pulse measured by FROG (see Methods), which indicates a FWHM pulse duration of 19 fs.

A temporal compression down to **19 fs** with 50 W of average power was achieved in a nonlinear compression stage that consists of a photonic crystal fibre (PCF) followed by chirped mirrors.

Few cycle pulse generation by means of soliton self-compression of Ho:YAG thin-disk laser pulses at 2 μm in an optical fiber

Multi-mW, few-cycle mid-infrared continuum spanning from 500 to 2250 cm^{-1}

Jinwei Zhang[1,*], Ka Fai Mak[1,*], Nathalie Nagl[2], Marcus Seidel[1], Dominik Bauer[3], Dirk Sutter[3], Vladimir Pervak[2], Ferenc Krausz[1,2] and Oleg Pronin[1]

Light: Science & Applications (2018) **7**, 17180; doi:10.1038/lsa.2017.180; published online 23 February 2018

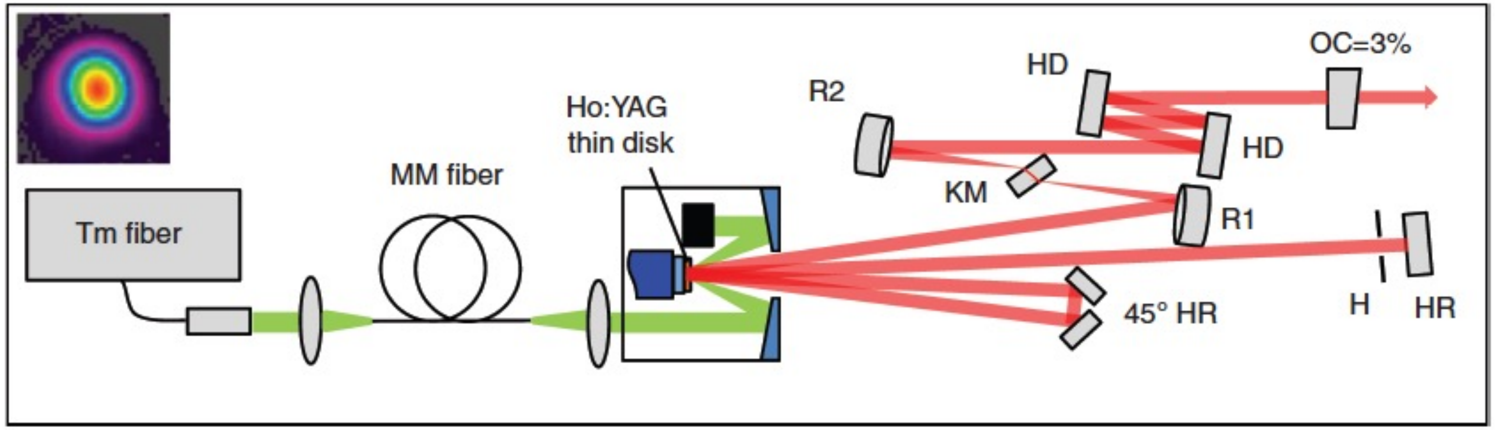

Laser: pulse duration 260 fs

Figure 1 Mode-locked Ho:YAG thin-disk oscillator. HR, high-reflection mirrors; R1 and R2, concave spherical mirrors; KM, Kerr medium; HD, high dispersion mirrors; H, hard aperture; OC, output coupler. The oscillator contains a wedged Ho:YAG thin disk with a thickness of ~200 μm and 2.5 at.% Ho doping, housed within a multi-pass pump head (TRUMPF Laser GmbH). The pump spot diameter on the thin disk is 2.5 mm. The thin disk is placed as a folding mirror in a cavity based on a Z-shaped design. A pair of 45° high-reflection mirrors folds the beam path to provide eight passes through the thin disk per round trip. A 1 mm-thick sapphire plate acting as the Kerr medium is placed at the focus between two concave mirrors (R1 and R2). The total anomalous group delay dispersion per round trip is −16000 fs^2, introduced by a pair of chirped mirrors with up to 4 bounces on each surface. A water-cooled copper plate with a circular hole is placed near an end mirror as a hard aperture to aid the stabilization of KLM. The total cavity length is ~1960 mm, corresponding to a repetition rate of 77 MHz. Inset: the beam profile of the oscillator output.

Few cycle pulse generation by means of soliton self-compression of Ho:YAG thin-disk laser pulses at 2 μm in an optical fiber

Silica-core photonic-crystal fiber (PCF) for spectral broadening and self compression

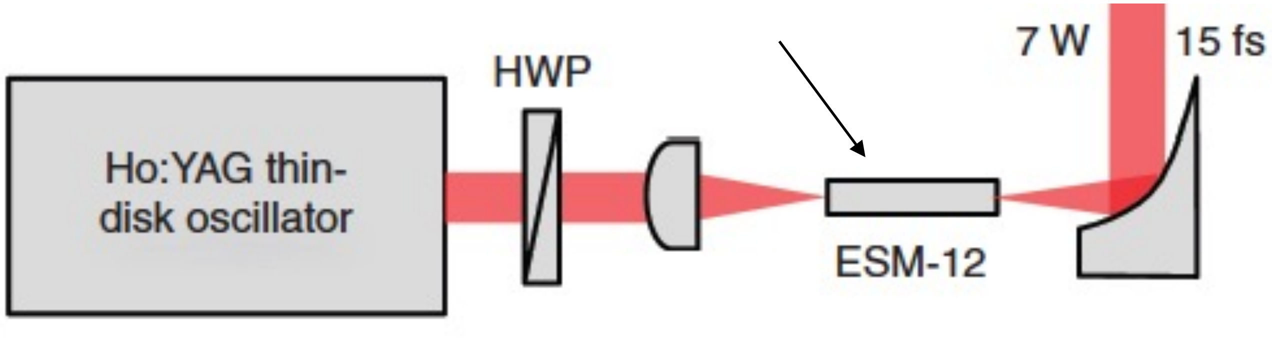

pulse duration 260 fs → **15 fs**
(self compression in a fiber)

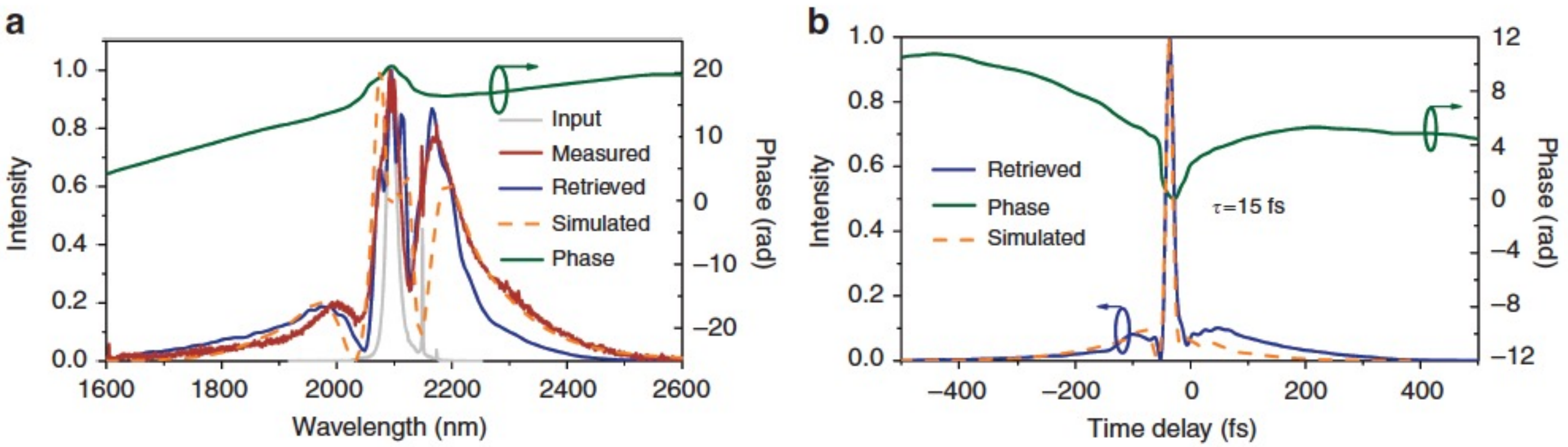

Self-focusing and defocusing nonlinearities

The consequences of self-focusing and defocusing nonlinearities in the time domain are analogous to those just described in the space domain. Just as in the space domain self-focusing led to energy localization in space, in the time domain localization occurs in time; i.e., the pulse width collapses.

The nonlinear Schrödinger equation

NLSE

$$\frac{\partial a}{\partial z} - \frac{i}{2}\beta_2 \frac{\partial^2 a}{\partial \tau^2} + i\gamma|a|^2 a = 0$$

$$\beta_2 = \frac{d^2 k}{d\omega^2}$$

$$\gamma = k_0 \frac{n_2}{A_{Eff}}$$

pulses broaden in time because of group velocity dispersion

pulses broaden in frequency because of self-phase modulation

The nonlinear Schrödinger equation describes the propagation of the wave through a nonlinear medium.

The second-order derivative represents the dispersion, while the last term represents the nonlinearity.

The equation models many nonlinearity effects in a fiber, including but not limited to self-phase modulation, four-wave mixing, second-harmonic generation, stimulated Raman scattering, optical solitons, ultrashort pulses, etc.